HHS Public Access

Author manuscript

Biochim Biophys Acta Gen Subj. Author manuscript; available in PMC 2021 November 01.

Published in final edited form as:

Biochim Biophys Acta Gen Subj. 2020 November ; 1864(11): 129697. doi:10.1016/j.bbagen.2020.129697.

MA-[D-Leu-4]-OB3, a small molecule synthetic peptide leptin mimetic, improves episodic memory, and reduces serum levels of tumor necrosis factor-alpha and neurodegeneration in mouse models of Type 1 and Type 2 Diabetes Mellitus

Zall Hirschstein[a], **Gautam Reddy Vanga**[b], **Guirong Wang**[b], **Zachary M. Novakovic**[a], **Patricia Grasso**[a]

[a]Albany Medical College, Albany, NY, USA,

[b]SUNY Upstate Medical University, Syracuse, NY, USA

Abstract

Background—Extracellular beta- amyloid (Aβ), intra-neuronal hyper-phosphorylated tau protein, and chronic inflammation are neuropathological hallmarks of Alzheimer's Disease (AD). A link between AD, insulin dysfunction, and tumor necrosis factor-alpha (TNF-α) in promoting both tau and Aß pathologies *in vivo* has been proposed.

Methods—MA-[D-Leu-4]-OB3 was given, with or without insulin, to streptozotocin (STZ)-treated male Swiss Webster mice, and to male diet-induced obese (DIO) mice. Brains were excised, and coronal sections were imaged with fluoro jade-C (FJC), thioflavin-S, or hematoxylin and eosin (H&E). Serum TNF-α and IGF-1 were measured by ELISA. Histopathological changes in the cerebral cortex (CC) and hippocampus (HC) were correlated with changes in glycemic regulation, episodic memory, and serum levels of TNF-α and IGF-1.

Results—In STZ-treated mice, blood glucose and serum TNF-α and IGF-1 were reduced by insulin alone, and normalized when MA-[D-Leu-4]-OB3 was given in combination with insulin. Improvement in episodic memory was inversely correlated with the number of FJC-positive cells in the CC and HC and serum TNF-a and IGF-1. FJC, thioflavin-S and H&E staining indicated no Aβ deposition. Similar results were observed in DIO mice treated with MA-[D-Leu-4]-OB3.

Corresponding author: Patricia Grasso, Ph.D., Department of Medicine, MC-141, Albany Medical College, 47 New Scotland Avenue, Albany, NY, 12208, USA, Telephone: 518-262-5639, Fax: 518-262 6303, grassop@amc.edu.

Author Contributions

Zall Hirschstein: Data curation; Formal analysis; Investigation; Software; Writing – review and editing

Gautam Reddy Vanga: Data curation; Formal analysis; Investigation; Software; Visualization; Writing – review and editing

Guirong Wang: Funding acquisition; Project administration; Resources; Supervision; Writing – review & editing

Zachary Novakovic: Conceptualization; Formal analysis; Writing – review & editing

Patricia Grasso: Conceptualization; Data curation; Formal analysis; Funding acquisition; Project administration; Resources; Supervision; Validation; Writing – original draft; Writing – review & editing

Compliance with Ethical Standards: Zall Hirschstein, Gautam Reddy Vanga, Guirong Wang, Zachary Novakovic, and Patricia Grasso declare that they have no conflict of interest.

Declarations of interest: none

Conclusions—The mechanism by which MA-[D-Leu-4]-OB3 improves episodic memory in mouse models of T1DM and T2DM appears to be related to improved insulin sensitivity and reduced TNF-α-induced neurodegeneration.

General Significance—MA-[D-Leu-4]-OB3 may have application to human pre-clinical and clinical AD and AD-like dementia by interrupting the cascade of insulin resistance, neuro-inflammation, and neurodegeneration, that characterizes these diseases.

Keywords

Alzheimer's Disease; Dementia; Episodic memory; Insulin resistance; Leptin peptides; Neurodegeneration

1. Introduction

Alzheimer's Disease (AD), as a distinct clinical entity, is currently defined by the identification of a specific neuropathological profile which includes the extracellular deposition of β-amyloid (Aβ) plaques, the formation of intra-neuronal neurofibrillary tangles (NTFs) consisting of aggregated, hyper-phosphorylated tau protein, and cytokine-mediated chronic inflammation (Duyckaerts et al., 2009; McCaulley and Grush, 2015; Jack et al., 2018). It is now generally accepted that tau pathology may be the primary driver of neurodegeneration in AD (Long and Holtzman, 2019), and that tumor necrosis factor alpha (TNF-α) plays a central role in the pathophysiology of this disease (Chang et al., 2017; Cavanagh and Wong, 2018). Data from both longitudinal and cross-sectional studies of tau- and amyloid-positron emission tomography (PET) imaging, combined with structural magnetic resonance imaging (MRI), confirm the presence of tau alone as sufficient for predicting cognitive impairment, and that deposition of Aβ is predictive of more severe tau-related-cognitive dysfunction (Aschenbrenner et al., 2018; Hanseeuw et al., 2019).

There is a growing body of evidence supporting links between AD, defective insulin signaling, and chronic inflammation (de Oliveira Santos et al., 2012; De Felice, 2013; De Felice and Ferreira 2014; El Khoury et al, 2014; Ferreira et al., 2018). In this regard, inflammation is a prominent feature of both AD and diabetes, and is thought to play a critical role in the pathogenesis of both disorders (Clark et al. 2012; Ferriera et al., 2014). It is also well known that TNF-α is overexpressed in obese individuals (Hotamisligil et al., 1995); that elevated TNF-α levels cause peripheral insulin resistance (Hotamisligil et al., 1996); and that brain inflammation is associated with the defective neuronal insulin signaling that is characteristic of AD (Bomfim et al., 2013).

Our laboratory has recently shown that MA-[D-Leu-4]-OB3, a small molecule synthetic peptide leptin mimetic, crosses the blood–brain barrier (Anderson et al., 2017), reduces body weight gain (Wang et al., 2018), improves insulin sensitivity (Wang et al., 2018; Anderson et al., 2019; Hirschstein et al., 2019), and normalizes episodic memory in mouse models of T1DM (Anderson et al., 2019) and T2DM (Hirschstein et al., 2019). In the present study, we hypothesized that the observed ability of MA-[D-Leu-4]-OB3 to improve cognitive function may be influenced not only by its effects on glycemic control, but also by actions associated with reducing serum concentrations of pro-inflammatory cytokines known to be associated

with neuronal degeneration. To test this hypothesis, the cerebral cortex and hippocampal regions of brains from untreated and MA-[D-Leu-4]-OB3-treated mouse models of T1DM (STZ-induced) and T2DM (diet-induced obese, DIO) were imaged and examined for signs of neurodegeneration and Aβ deposition. Serum levels of the pro-inflammatory cytokines TNF-α and IGF-1 were measured.

The objective of these efforts was to identify a correlation, if any, between the previously observed effects of MA-[D-Leu-4]-OB3 on glycemic regulation and episodic memory with histopathological changes in the brain, and changes in serum levels of pro-inflammatory cytokines known to influence neurodegeneration. Our results suggest that the mechanism by which MA-[D-Leu-4]-OB3 has been shown to improve episodic memory in two models of AD-like cognitive dysfunction may be related not only to its ability to improve insulin sensitivity peripherally and in the brain, but also to reduce TNF-α-induced neurodegeneration.

2. Materials and Methods

2.1. Animal procedures

2.1.1. Animals and housing

2.1.1.1. T1DM mouse model: Four- to five- week old male Swiss Webster (SW) mice were obtained from Taconic Farms (Germantown, NY, USA). Upon arrival, the mice were randomized by weight into four treatment groups (n = 8 mice per group): Group 1: normal SW controls (to receive vehicle alone); Group 2: STZ-treated SW (to receive vehicle alone); Group 3: STZ-treated SW (to receive insulin alone); Group 4: STZ-treated SW (to receive insulin + MA-[D-Leu-4]-OB3). The mice were housed in polycarbonate cages fitted with stainless steel wire lids and air filters in the Albany Medical College Animal Resources Facility. The mice were maintained at a constant temperature (24° C) with lights on from 07:00 to 19:00 h, and allowed food and water ad libitum.

2.1.1.2. T2DM mouse model: Nine week-old male C57BL/6J wild type mice (B6DIOCONTROL-M) placed on a low fat diet after weaning, and diet-induced obese mice (DIO-B6-M) placed on a high-fat diet at six weeks of age, were obtained from Taconic Farms (Germantown, NY, USA). Upon arrival, the mice were randomized by weight into three treatment groups (n = 8 mice per group): Group 1: C57BL/6J wild-type controls on low-fat diet (to receive vehicle alone); Group 2: DIO mice on high-fat diet (to receive vehicle alone); Group 3: DIO mice on high-fat diet (to receive MA-[D-Leu-4]-OB3). The mice were housed in polycarbonate cages fitted with stainless steel wire lids and air filters in the Albany Medical College Animal Resources Facility. The mice were maintained at a constant temperature (24° C) with lights on from 07:00 to 19:00 h, and allowed food and water ad libitum.

2.1.2. Feeding and weighing schedule

2.1.2.1. T1DM mouse model: On day zero of the study, between 8:00 and 9:00 h, the mice received approximately 400 g (tared) of pelleted rodent diet (Prolab Rat, Mouse, Hamster 3000, St. Louis, MO, USA), composed of 22 kcal % crude protein, 5 kcal % crude

fat, 5 kcal % fiber, 6 kcal % ash, 2.5 kcal % additional minerals, and containing 3.15 kcal/g. Plastic water pouches (tared) containing approximately 350 mL of water were added to each cage. Tared aliquots of food and water were added to the cages as needed throughout the 17-day testing period. To assure fasting (6 h) glucose levels on days in which blood glucose was measured, food was removed from the cages between 8:00 and 9:00 h, and replaced immediately after testing. The mice were weighed daily between 8:00 and 9:00 h on an Acculab V-333 electronic balance (Cole-Parmer, Vernon Hills, IL, USA).

2.1.2.2. T2DM mouse model: Upon arrival, C57BL/6J wild type mice received standard rodent chow composed of 22 kcal % protein, 5 kcal% fat, 5% fiber, 6% ash, 2.5% minerals, and containing 3.16 kcal per gram (Prolab* Isopro* RHM 3000, Prolab, St. Louis, MO, USA). DIO mice received rodent chow composed of 20 kcal% protein, 20 kcal% carbohydrate, 60 kcal% fat, and containing 5.24 kcal per gram (D12492, Research diets, New Brunswick, NJ, USA). C57BL/6J wild type mice received approximately 400 g (tared) of standard rodent chow (low-fat), and DIO mice received approximately 400 g (tared) of the high-fat diet. Tared water pouches containing approximately 350 mL of water were placed on each cage. Food and water (tared) were added to the cages as needed.

To assure six-hour fasting glucose levels on days in which blood glucose was measured, food was removed from the cages between 08:00 and 09:00 h and replaced immediately after testing. When oral glucose tolerance tests (OGTTs) were done, overnight fasts (16 h) were initiated by removing food from the cages between 17:00 and 18:00 hours the afternoon before testing. OGTTs were performed between 09:00 and 10:00 the following day. The mice were weighed weekly on an Acculab V-333 electronic balance (Cole-Parmer, Vernon Hills, IL, USA).

2.1.3. Streptozotocin (STZ) administration

2.1.3.1. T1DM mouse model: Three groups (n = 8 per group) of male SW mice were rendered hyperglycemic with two injections (ip) of 100 mg/kg STZ in 100 μL phosphate buffered saline (PBS) given 24 h apart. The control group (n = 8) was given 100 μL PBS (ip). Fasting (6 h) blood glucose levels were measured prior to STZ treatment to establish baseline glucose levels. To avoid the metabolic stress of repeated daily fasting, non-fasting glucose was measured each day thereafter to assess the progression of hyperglycemia resulting from STZ treatment. Insulin treatment, in the absence or presence of MA-[D-Leu-4]-OB3, was initiated when non-fasting blood glucose levels in STZ-treated mice were elevated 100 to 200 mg/dL higher than those of normal mice.

2.1.4. Insulin and MA-[D-Leu-4]-OB3 administration

2.1.4.1. T1DM mouse model: A detemir insulin delivery pen (Levemir®, Novo Nordisk, Malov, Denmark) was used to prepare a solution of 0.05 U insulin/100 μL PBS, which was delivered by subcutaneous (sc) injection once daily between 16:00 and 17:00 h for 17 days. MA-[D-Leu-4]-OB3 was prepared commercially as a C-terminal amide by Atlantic Peptides (Lewisburg, PA, USA). MA-[D-Leu-4]-OB3 (mw 944), an analog of [D-Leu-4]-OB3 (Ser-Cys-Ser-dLeu-Pro-Gln-Thr, mw 734), is a synthetic linear peptide amide conjugated at the N-terminus to a myristic (tetra-decanoic) acid moiety. MA-[D-Leu-4]-OB3 was dissolved in

0.3% dodecyl maltoside (DDM, Intravail®, Aegis Therapeutics, San Diego, CA, USA) reconstituted in sterile deionized water, and delivered by gavage once daily at a concentration of 16.6 mg/kg/100 μL DDM between 16:00 and 17:00 h for 17 days.

2.1.4.2. T2DM mouse model: After 30 weeks on their respective diets, wild type C57BL/6J mice on the low-fat diet and one group of DIO mice on the high-fat diet received vehicle only, while the other group of DIO mice on the high-fat diet received MA-[D-Leu-4-]-OB3 for 14 days. MA-[D-Leu-4]-OB3 was dissolved in vehicle (0.3% dodecyl maltoside, DDM, trade name Intravail®, Aegis Therapeutics, San Diego, CA, USA, reconstituted in sterile deionized water), and delivered by oral gavage once daily at a concentration of 16.6 mg/kg/100 μL DDM between 16:00 and 17:00. No undesirable side effects were noted in MA-[D-Leu-4]-OB3- or vehicle-treated control mice throughout the entire course of the study.

2.1.5. Blood glucose measurement

2.1.5.1. T1DM and T2DM mouse models: Both fasting (6 h) and non-fasting blood samples were drawn by snipping the tip of the tail of each mouse. The blood droplet formed at the tip was applied to a glucose test strip. Glucose levels were measured with a OneTouch Verio IQ glucose meter (Janssen Pharmaceuticals, Raritan, NJ, USA).

2.1.5.2. T2DM mouse model: Oral glucose tolerance testing: Following an overnight fast (16 h), the mice received a single dose of 100 μL DDM (vehicle) alone or MA-[D-Leu-4]-OB3 (16.6 mg/kg) in 100 μL DDM. After 60 minutes, blood glucose levels were measured (as described in 2.1.5.1) and the mice were challenged with 100 μL D-glucose (2g/kg) in phosphate-buffered saline (PBS). Additional glucose measurements were taken at 15, 30, 45 and 60 minutes after the glucose challenge.

2.1.6. Novel object behavioral testing

T1DM and T2DM mouse models: Novel object recognition testing, as described by Bevins and Besheer (2006), was done after 17 days (T1DM mouse model) and 14 days (T2DM mouse model) of treatment with MA-[D-Leu-4]-OB3.

2.1.6.1. Apparatus and environment: In a designated behavioral testing room, a square black plastic chamber with smooth walls and floor, and divided into four equal quadrants 51 cm long × 51 cm wide × 38 cm high, was thoroughly cleaned with 70% ethanol. Overhead lights were turned off, and floor lamps with red bulbs were placed at the sides of the chamber so that red lighting was evenly distributed over the four quadrants. A Logitech HD Pro Webcam C920 (Logitech Inc., Newark, CA, USA) video camera with an adjustable zoom lens was mounted on an overhead bracket facing straight down over the center of the chamber. Habituation, training, and testing phases, each 5 minutes long, were recorded with an automated video tracking system (ANY-maze 6.06, Stoelting, IL, USA).

2.1.6.2. Protocol: Object selection and placement: Prior to novel object testing, the mice had been handled for approximately 15 minutes daily throughout the course of both studies. To habituate the mice to the testing environment, each mouse was placed in an empty

quadrant 24 hours before the training and testing phases, and allowed to freely explore for 5 minutes. During the training phase, the mice were exposed to two identical multi-colored Lego towers (familiar objects), approximately 5 cm high and 5 cm in diameter. These objects were placed in the center of each quadrant, equidistant from each other and from the quadrant walls. The mice were placed midway between the two objects with their noses pointing forward, and allowed to explore the objects for 5 minutes. In the testing phase, one of the Lego towers was replaced with a multi-colored rubber duckling (novel object), approximately 6 cm high and 6 cm long. The objects were placed in the center of each quadrant equidistant from each other and from the quadrant walls. As in the training phase, mice were placed midway between the two objects with their noses pointed forward, and allowed to explore these objects for 5 minutes. Approximately one hour separated the training phase from the testing phase, during which time the mice were returned to their home cages. The chamber was cleaned with 70% ethanol after each 5-min habituation/training/testing period.

2.1.6.3. Scoring: The videos from the training and the testing phases were blinded and then manually scored. The exploration time of both novel and familiar objects was defined as the time a mouse interacted with an object, i.e., when the mouse's nose touched the object or was within 1 cm of the object and pointed directly at the object. Not counted as exploration: when the mouse climbed on top of the object or was not approaching the object. For each mouse, the novel object and familiar object exploration times (in seconds) were recorded, and the discrimination index (DI) was calculated as follows: time (in seconds) exploring the novel object minus time (in seconds) exploring the familiar object divided by the total time (in seconds) exploring the novel object and familiar object × 100.

2.1.7. Blood collection and serum preparation—

At the end of both studies (T1DM study: mouse age 6.5 weeks; T2DM study: mouse age 41 weeks), the mice were anesthetized with isoflurane (5%) and exsanguinated by cardiac puncture. Euthanasia was confirmed by cervical dislocation. The blood was collected in sterile non-heparinized plastic centrifuge tubes and allowed to stand at room temperature for 1 h. Individual serum samples were prepared by centrifugation for 30 min at 2000 × g in an Eppendorf 5702R, A-4–38 rotor (Eppendorf North America, Westbury NY, USA). The serum samples from each experimental group were then pooled and stored frozen at −20 C until analyzed for TNF-α and IGF-1 content.

2.1.8. Tissue preparation

2.1.8.1. T1DM and T2DM mouse models: Following exsanguination by cardiac puncture, the chest cavities were opened, and whole body fixation was achieved by transcardiac perfusion at 5 mL/min with normal saline (0.5 mL/g BW) through the left ventricle, followed by 4% phosphate-buffered paraformaldehyde perfusion (1 mL/g BW). Brains were excised, post-fixed in paraformaldehyde (4%) at 4°C for 4 h, and cryo-protected in 30% sucrose at −20°C until processed for histochemical analysis.

All of these animal procedures were approved by the Albany Medical College Animal Care and Use Committee, and were performed in accordance with relevant guidelines and

regulations as outlined in the Guide for the Care and Use of Laboratory Animals, Eighth edition (2011). (http://grants.nih.gov/grant/olaw/guide-for-the-care-and-use-oflaboratory-animals.pdf).

2.2. Histochemical analysis

2.2.1. T1DM mouse model—Coronal brain sections (3 mm thick) were paraffin imbedded. Five-micron thick sections were then cut on a Spencer Precision rotary microtome (American Optical, Southbridge, MA, USA), mounted on polysine microscope adhesion slides (Thermo Fisher Scientific, Waltham, MA, USA), and stained with a ready-to-dilute Fluoro-jade C (FJC) staining kit (Biosensis, Temecula, CA, USA) and DAPI (Sigma Aldrich, St. Louis, MO, USA), according to instructions supplied by the manufacturer. The slides were cover-slipped with a neutral mounting medium, DPX (Sigma-Aldrich, St. Louis, MO, USA), and imaged on a Nikon Eclipse TE2000-U inverted microscope (Nikon Instruments, Mellville, NY, USA) under blue light. FJC-positive cells in 10 different fields within the cerebral cortex, and 10 within the CA-1 region and DG of the hippocampus of brains from four mice in each treatment group were counted manually and expressed as number of FJC-positive cells per field.

Similarly, 5-micron thick coronal sections of brains from three or four mice in each treatment group were stained with hematoxylin and eosin (H&E) and examined for evidence of Aβ deposition by light microscopy.

2.2.2. T2DM model—35-micron free-floating frozen coronal sections were cut on a Leica CM 3050 cryostat (Leica Biosystems Inc., Buffalo Grove, IL, USA) and transferred to Net Well inserts (Sigma-Aldrich, St. Louis, MO, USA) in 12-well plastic tissue culture dishes. The sections were washed with phosphate buffered saline (PBS), stained with thioflavin-S (Sigma Aldrich, St. Louis, MO, USA) and DAPI (Sigma Aldrich, MO, USA), mounted with Cytoseal 60 (Richard-Allan Scientific, Kalamazoo, MI, USA) on Super-Frost Plus glass slides (Fisher Scientific, Pittsburgh, PA, USA), and covered with glass coverslips. The slides were stored in light-proof slide boxes and imaged on a Zeiss Axiovert 200 inverted microscope (Carl Zeiss Microscopy, LLC, White Plains, NY, USA).

2.3. TNF-α and insulin-like growth factor-1 (IGF-1) measurement: T1DM and T2DM mouse models

The TNF-α and IGF-1 content in pooled serum samples from each experimental group (8 animals per group) was measured using mouse enzyme linked immunosorbent assay (ELISA) kits obtained from RayBiotech (Peachtree Corners, GA, USA) according to the instructions supplied by the manufacturer.

2.4. Statistical analysis

All data are expressed as mean ∓ SEM. SigmaPlot®12.5 for windows (SPSS, Chicago, IL. USA) was used to determine statistical significance. Differences in blood glucose levels, discrimination index, numbers of FJC-positive cells, and serum levels of TNF-α and IGF-1 were compared by one-way analysis of variance (ANOVA), followed by *post hoc* analysis using the Holm-Sidak method. Differences between groups were considered statistically

significant when $P < 0.05$. Both of these studies were done twice. The data were not pooled, and represent the results of a single study.

3. Results

3.1. Effects of MA-[D-Leu-4]-OB3 on glycemic control in male STZ-treated Swiss Webster (SW) and C57BL/6J diet-induced obese (DIO) mice

The effects of MA-[D-Leu-4]-OB3 in mouse models of T1DM and T2DM on glycemic control are summarized in Table 1. In STZ-treated male Swiss Webster mice (T1DM model), insulin treatment alone for 17 days reduced, but not significantly, fasting blood glucose levels. When MA-[D-Leu-4]-OB3 was given in combination with insulin, fasting glucose was reduced to levels approximating those of normal SW mice ($P > 0.05$). In male C57BL/6J mice maintained on a high-fat diet for 30 weeks (T2DM model), glucose tolerance was significantly ($P < 0.05$) impaired by high-fat diet alone. After 14 days of treatment with MA-[D-Leu-4]-OB3, glycemic regulation was restored, and glucose tolerance was equivalent ($P > 0.05$) to that of C57BL/6J mice of the same age and sex maintained on a low-fat diet for 30 weeks.

3.2. Effects of MA-[D-Leu-4]-OB3 on episodic memory in STZ-treated male SW and C57BL/6J DIO mice

The effects of MA-[D-Leu-4]-OB3 on episodic memory, described by changes in discrimination index (DI), in male STZ-treated SW mice given insulin alone or in combination with MA-[D-Leu-4]-OB3 for 17 days, and in male C57BL/6J DIO mice given MA-[D-Leu-4]-OB3 for 14 days, are shown in Fig. 1A and Fig. 1B, respectively. Episodic memory was significantly ($P < 0.05$) impaired by STZ treatment, only partially restored by insulin alone, but normalized ($P > 0.05$) when insulin was given in combination with MA-[D-Leu-4]-OB3 (Fig 1A). Similar results were observed in male C57BL/6J DIO mice maintained on a high-fat diet for 30 weeks (Fig. 1B). Episodic memory, significantly ($P < 0.05$) impaired by prolonged exposure to the high-fat diet alone, was normalized ($P > 0.05$) after 14 days of treatment with MA-[D-Leu-4]-OB3.

3.3. Effects of MA-[D-Leu-4]-OB3 on neurodegeneration in STZ-treated SW mice

Fluoro-jade C (FJC) was used to examine the effects of MA-[D-Leu-4]-OB3 on neurodegeneration in male STZ-treated SW mice (Fig. 2). As expected, little to no FJC labeling in the cerebral cortex (Fig. 2A) was observed in normal SW mice. In contrast, STZ-treated mice exhibited multiple FJC stained neurons and fibers in these brain regions (Fig. 2B). Treatment with insulin alone for 17 days significantly reduced FJC staining in the cerebral cortex (Fig. 2C). When MA-[D-Leu-4]-OB3 was given in combination with insulin, very little or no labeling was evident (Fig. 2D). Similar changes in the level of FJC staining were observed in the dentate gyrus and CA1 region of the hippocampus (images not shown). Quantification of the number of FJC-positive cells in multiple fields (10) of the cerebral cortex and hippocampus is shown in Fig. 3A and Fig. 3B, respectively.

3.4. Effects of STZ and high-fat diet on Aβ deposition in male STZ-treated SW and C57BL/6J DIO mice

Thioflavin-S and hematoxylin and eosin (H&E) staining were used in efforts to image Aβ deposition in male STZ-treated SW and C57BL/6J DIO mice.In both models, no evidence of Aβ plaques could be identified by either staining protocol (images not shown), or in the FJC-stained images (Fig. 2).

3.5. Effects of MA-[D-Leu-4]-OB3 on serum TNF-α and IGF-1 levels in male STZ-treated Swiss Webster and C57BL/6J DIO mice

The effects of MA-[D-Leu-4]-OB3 on TNF-a levels in STZ-treated SW mice given insulin alone or in combination with MA-[D-Leu-4]-OB3, and in DIO mice maintained on a high-fat diet are shown Fig 4. STZ significantly ($P < 0.05$) elevated serum TNF-a levels, which were significantly ($P < 0.05$) reduced by insulin alone. When MA-[D-Leu-4]-OB3 was given in combination with insulin, serum TNF-α levels were reduced to levels equivalent to ($P > 0.05$) those of normal SW mice (Fig. 4A). Similarly, serum TNF-a was significantly ($P < 0.05$) elevated in DIO mice maintained on a high-fat diet, and treatment with MA-[D-Leu-4]-OB3 reduced serum TNF-α to levels equivalent to those seen in normal C57BL/6J mice of the same age and sex maintained on the low-fat diet (Fig. 4B).

The effects of MA-[D-Leu-4]-OB3 on serum IGF-1 levels in STZ-treated SW mice given insulin alone or in combination with MA-[D-Leu-4]-OB3, and in DIO mice maintained on a high-fat diet are shown in Fig. 5A and Fig. 5B, respectively. STZ treatment significantly ($P < 0.05$) elevated serum IGF-1 levels which were reduced ($P < 0.05$) by Insulin alone. When given in combination with insulin, MA-[D-Leu-4]-OB3 further reduced ($P < 0.05$) serum IGF-1 to levels lower than those seen in normal SW mice (Fig. 5A). In male DIO mice, serum IGF-1 was significantly ($P < 0.05$) elevated by maintenance on a high-fat diet for 30 weeks. Treatment with MA-[D-Leu-4]-OB3 normalized serum IGF-1 to levels equivalent ($P > 0.05$) to those of normal C57BL/6J mice of the same age and sex maintained on a low-fat diet. (Fig. 5B)

4. Discussion

One of many challenges associated with developing a preventative therapy for the treatment of AD is the identification of early biomarkers of this disease. There is no doubt that characterization of the preclinical stages of AD would provide a target for therapeutic attack on its progression or prevention. Human data indicate that AD is a long pathological process that may start decades before the onset of clinical cognitive decline. Several preclinical stages of AD have been proposed, and are currently characterized by studying changes in imaging modalities (Cavanagh and Wong, 2018), biomarkers including beta amyloid and tau levels in cerebrospinal fluid (CSF) (Sperling et al., 2011), and serum levels of pro-inflammatory cytokines (De Felice and Ferriera, 2014).

In this regard, links between defective insulin signaling, AD, and inflammation are well-established (de Oliveira Santos et al., 2012; Ferreira et al., 2014; El Khoury et al., 2014; De Felice and Ferreira, 2014; Ferreira et al., 2018). The observed ability of MA-[D-Leu-4]-OB3

to improve insulin sensitivity peripherally and in the brain, and to enhance episodic memory in mouse models of both T1DM (Anderson et al., 2019) and T2DM (Hirschstein et al., 2019), prompted us to expand our investigation of the actions of MA-[D-Leu-4]-OB3 to include an examination of its effects on the modulation of one or more pro-inflammatory cytokines known to enhance neurodegeneration, and on histopathological changes in the hippocampus and cerebral cortex in these mouse models.

To this end, we examined the influence of MA-[D-Leu-4]-OB3 on serum levels of TNF-a, a pro-inflammatory cytokine known to play a central role in the pathophysiology of AD (Chang et al., 2017; Cavanagh and Wong, 2018), in mouse models of insulin deficiency (STZ-treated SW mice) and insulin resistance (C57BL/6J DIO mice). In both models, the ability of MA-[D-Leu-4]OB3 to (1) improve fasting blood glucose levels and glucose tolerance, (2) reduce STZ- and high-fat diet-associated neurodegeneration, and (3) normalize STZ- and high-fat diet-associated elevation in serum TNF-α levels, was positively correlated with its ability to improve episodic memory.

Worthy of special note, although FJC labeling revealed the presence of severe neurodegeneration in STZ-treated mice, and contrary to what might be expected based on their metabolic (insulin resistance), serologic (high TNF-α and IGF-1 levels), and behavioral (low DI) profiles, no Aβ deposition could be visualized in their brains by FJC, H&E or thioflavin S staining. Absence of Aβ deposition was also observed in the brains of untreated C57BL/6J DIO mice with similar metabolic, serologic, and behavioral profiles. These observations suggest that although cognitive function was significantly impaired in both models, these deficits may be early-onset, and more than likely, will be amplified with time and future Aβ deposition.

We also noted that neurodegeneration, identified by the presence of FJC-positive neurons, was more prominent in the cerebral cortex than in the hippocampus of STZ-treated mice not receiving insulin alone, or insulin in combination with MA-[D-Leu-4]-OB3. Our findings are consistent with those of a recent study which showed that tau pathology in AD-associated cognitive impairment in humans is brain region-specific and only weakly related to amyloid burden, and that episodic memory deficits are mediated, at least in part, by grey matter atrophy in the lateral and medial parietal cortex (Bejanin et al., 2017).

Our results are in agreement with what has been reported in a transgenic mouse model of AD which indicated that increased hippocampal levels of TNF-α and enhanced excitatory synaptic transmission are early-onset changes that occur weeks before amyloid plaque formation was detected (Cavanagh et al., 2016). More importantly, this study and a subsequent paper by Cavanagh and Wong (2018) indicated that inhibiting plaque formation not only normalized excitatory synaptic function, but actually prevented future impairment of cognitive function.

Although the role of IGF-1 in brain health and function has not been clearly defined and is not without controversy, it is well known that serum IGF-1 levels are elevated in response to brain injury (Labandeira-Garcia et al., 2017), and also increase TNF-α expression (Renier et al., 1996). Because our histopathological and behavioral evidence indicated that severe

neurodegenerative changes were associated with both STZ treatment and prolonged maintenance on a high-fat diet, we were interested in determining whether or not the observed damage was reflected in changes in serum IGF-1, and if treatment with MA-[D-Leu-4]-OB3 modulated serum IGF-1 concentrations. In both models, treatment with MA-[D-Leu-4]-OB3 resulted in lower or normalized IGF-1 levels, reduced histopathological evidence of neurodegeneration, and improved episodic memory.

In conclusion: based on the established links between diabetes, inflammation, and AD-like cognitive dysfunction, and the ability of MA-[D-Leu-4]-OB3 to increase insulin sensitivity, modulate serum levels of TNF-α and IGF-1, and improve cognitive function, it seems reasonable to suggest a possible application of MA-[D-Leu-4]-OB3 for the treatment of preclinical AD or other AD-like dementias, such as vascular dementia (VaD) or mixed dementia, in individuals diagnosed as pre-diabetic and/or those with elevated serum or CSF levels of TNF-α and/or IGF-1. In this regard, given the strong linkage between diabetes and AD, the presence of prediabetes may be considered a “preclinical metabolic biomarker” for AD-like cognitive dysfunction. By slowing or preventing its progression to full-blown diabetes while reducing TNF-α and IGF-1 levels, intervention with MA-[D-Leu-4]-OB3 may be able to “nip AD and AD-like dementia in the bud”, thus interrupting the cascade of insulin resistance in the brain, neuro-inflammation, neurodegeneration, and synaptic dysfunction that characterize clinical AD and AD-like dementias. Exploring the mechanism(s) by which MA-[D-Leu-4]-OB3 modulates this complex network of metabolic, immunologic, and neurologic pathways will be the efforts of future studies.

Acknowledgments

This research was supported by a grant from the Willard B. Warring Memorial Fund, Albany Medical College, Albany, NY, USA (P.G.), and in part by the National Institutes of Health (grant number R01HL136706 (G.W.). The Intravail® reagent was graciously provided by Aegis Therapeutics, San Diego, CA, USA.

References

Anderson BM, Jacobson L, Novakovic ZM, Grasso P (2017) Oral delivery of [D-Leu-4]-OB3 and MA-[D-Leu-4]-OB3, synthetic peptide leptin mimetics: immunofluorescent localization in the mouse hypothalamus. Brain Res 1664, 1–8. doi: 10.1016/j.brainres.2017.03.020 [PubMed: 28347670]

Anderson BM, Hirschstein Z, Novakovic ZM, Grasso (2019) MA-[D-Leu-4]-OB3, a small molecule synthetic peptide leptin mimetic, mirrors the cognitive enhancing action of leptin in a mouse model of Type 1 Diabetes Mellitus and Alzheimer’s Disease-like cognitive impairment. Int J Pep Res Thera doi:10.1007/s10989-019-09929-w

Aschenbrenner AL, Gordon BA, Benzinger TLS, Morris JC, Hassenstab JJ (2018) Influence of tau PET, amyloid PET, and hippocampal volume on cognition in Alzheimer’s disease. Neurology 91, e859–e866. doi: 10.1212/WNL.0000000000006075 [PubMed: 30068637]

Bejanin A, Schonhaut DR, La Joie R, Kramer JH, Baker SL, Sosa N, Ayakta N, Cantwell A, Janabi M, Lauriola M, O’Neil JP, Gorno-Tempini ML, Miller ZA, Rosen HJ, Miller BL, Jagust MJ, Rabbinovici GD (2017) Tau pathology and neurodegeneration contgribuite to cognitive impairment in Alzheimer’s disease. Brain 140, 3286–3300. doi:10.1093/brain/awx243 [PubMed: 29053874]

Bevins RA, Besheer J (2006) Object recognition in rats and mice: a one-trial non-matching-to-sample learning task to study‘recognition memory’. Nat Protoc 1, 1306–1311. 10.1038nprot.20062095 [PubMed: 17406415]

Bomfim TR, Fomy-Germano L, Sathler LB, Brito-Moreira J, Houzel JC, Decker H, Silverman MA, Kazi H, Melo HM, McClean PL, Holscher C, Arnold SE, Talbot K, Klein WL, Munoz DP, Ferreira ST, De Felice FG (2012) An Anti-diabetes agent protects the mouse brain from defective insulin signaling caused by Alzheimer's disease-related Aβ oligomers. J Clin Invest 122, 1339–1353. doi:10.1172/JCI57256 [PubMed: 22476196]

Cavanagh C, Tse YC, Nguyen HB, Krantic S, Breitner JC, Wong R. (2016) Inhibiting tumor necrosis factor-alpha before amyloidosis prevents synaptic deficits in an Alzheimer's disease model.Neurobiol Aging 47, 41–49. doi: 10.1016/j.neurobiolaging.2016.07.009 [PubMed: 27552480]

Cavanagh C, Wong TP (2018) Preventing synaptic deficits in Alzheimer's disease by inhibiting tumor necrosis factor alpha signaling. IBRO Reports 4, 18–21. doi: 10.1016/j.ibror.2018.01.003 [PubMed: 30135948]

Chang R, Yee K-L, Sumbria RK (2017) Tumor necrosis factor α inhibition for Alzheimer's Disease. J Cent Ner Sys Dis 9,1–5. doi: 10.1177/1179573517709278

Clark I, Atwood C, Bowewnm R, Paz-Filho G, Vissel (2012) Tumor necrosis factor-induced cerebral insulin resistance in Alzheimer's disease links numerous treatment rationales. Pharmacol Rev 64, 1004–1026. doi: 10.1124/pr.112.005850 [PubMed: 22966039]

DeFelice FG (2013) Alzheimer's Disease and insulin resistance: translating basic science into clinical applications. J Clin Invest 123, 531–539. doi: 10.1172/JCI64595 [PubMed: 23485579]

DeFelice FG, Ferriera ST (2014) Inflammation, defective insulin signaling, and mitochondrial dysfunction as common molecular denominators connecting type 2 diabetes to Alzheimer Disease. Diabetes 63, 2263–2272. doi: 10.2337/db13-1954

De Oliveira Santos T, Mazucanti CHY, Xavier GF, Da Silva Torrao A(2012) Early and late neurodegeneration and memory disruption after intracerebroventricular streptozotozin. Physiol Behav 107, 401–413. doi: 10.1016/j.physbeh.2012.06.019 [PubMed: 22921433]

Duyckaerts C, Delatour B, Potier (2009) Classification and basic pathology of Alzheimer's disease. Acta Neuropathol 118,5–36. doi: 10.1007/s00401-009-0532-1 [PubMed: 19381658]

El Khoury NB, Gratuze M, Papon MA, Bretteville A, Panel E (2014)Insulin dysfunction and Tau pathology. Front Cell Neurosci 8, 1–18. doi: 10.3389/fncel.2014.00022 [PubMed: 24478626]

Ferreira LSS, Fernandes CS, Vieira MNN, De Felice FG (2018) Insulin resistance in Alzheimer's Disease. Front Neurosci 12, 1–11 doi:10.3389/fnins.2018.00830 [PubMed: 29403346]

Ferreira ST, Clarke JR, Bomfim TR, De Felice FG(2014) Inflammation, defective insulin signaling, and neuronal dysfunction in Alzhimer's disease. Dement 10, S76–S83. doi: 10.1016/j.jalz.2013.12.010

Giannakopoulos P, Hermann FR, Bussiere T, Bouras C, Kovario E, Perl DP, Morriswon JH, Gold G, Hof PR (2003) Tangle and neuron numbers, but not amyloid load, predict cognitive status in Alzheimer's Disease. Neurology 60, 1495–1500. doi: 10.1212/01.wnl.0000063311.58879.01 [PubMed: 12743238]

Hanseeuw BJ, Betensky RA, Jacobs HIL, Schultx AP, Sepulcre J, Becker JA, Cosio DMOP, Farrell M, Quiroz YT, Mormino EC, Buckley RF, Papp KV, Amariglio RA, Dewachter I, Ivanoiu A, Huijbers W, Hedden T, Marshall GA, Chhatwal JP, Rentz DM, Sperling RA, Johnson K (2019) Association of amyloid and tau with cognition in preclinical Alzheimer Disease. Alongitudinal study. JAMA Neurol 10.1001/jamaneurolo.2019.1424

Hirschstein Z, Novakovic ZM, Grasso P (2019) MA-[D-Leu-4]-OB3, a small molecule synthetic peptide leptin mimetic, normalizes glucose tolerance and episodic memory in amouse model of Type 2 Diabetes Mellitus and Alzheimer's Disease-Like Cognitive Impairment. Int J Pep Res Thera doi: 10.1007/s10989-019-09995-0

Hotamisligil GS, Arner P, Caro FJ, Atkinson RI, Spiegelman BM (1995) Increased adipose tissue expression of tumor necrosis factor-alpha in human obesity and insulin resistance. J Clin Invest 95, 2409–2415. doi: 10.1172/JCI117936 [PubMed: 7738205]

Hotamisligil GS, Peraldi P, Budavari A, Elllis R, White MF, Spiegelman BM (1996) IRS-1-mediated inhibition of insulin receptor tyrosine kinase activity in TNF-alpha and obesity-induced insulin resistance. Science 271, 665–668. doi: 10.1126/science.271.5249.665 [PubMed: 8571133]

Jack CR Jr, Bennett DA, Blennow K, Camillo MC, Dunn B, Haeberlwin SB, Holtssman DM, Jagust W, Jessen F, Karlawish J, Liu E, Molinuevo JL, Montine T, Phelps C, Rankin KP, Rowe CC, Scheltens P, Siemers E, Snyder HM, Sperling R (2018) NIA-AA Research Framework: Toward a biological definition of Alzheimer's Disease. Alzheimers Dement 14, 535–562. doi: 10.1016/j.jalz.2018.02.018 [PubMed: 29653606]

Kinney JW, Bemillerr SM, Murtishaw AS, Leisgang AM, Salazar AM, Lamb BT (2018) Inflammation as a central mechanism in Alzheimer's disease. Alzheimer's & Dement 4, 575–560. doi: 10.1016/j.trci.2018.06.014

Labandeira-Garcia JL, Costa-Besada MA, Labandeira CM, Villar-Cheda B, Rodriguewz-Perez AI (2017) Insulin-like growth factor-1 and Neuroinflammation. Fron Aging Neurosci doi: 10.3389/fragi.2017.00365

Long JM, Holtzman DM (2019) Alzheimer Disease: an update on pathobiology and treatment strategies. Cell 179, 312–339. doi: 10.1016/j.cell.2019.09.001 [PubMed: 31564456]

McCaulley ME, Grush KA (2015) Alzheimer's disease: exploring the role of inflammation and implications for treatment. Int J Alzheimers Dis 2015, 515248.doi: 10.1155/2015/515248 [PubMed: 26664821]

Nelson PT, Alafuzoff I, Bigio EH, Bouras C, Braak H, Cairns NJ, Castellaniu RJ, Crain BJ, Davies P, Del Tredici K, Duyckaerts C, Frosch MP, Haroutunian V, Hof PR, Hulette CM, Hyman BT, Iwatsubo T, Jellinger KA, Jicha GA, Kövari E, Kukull WA, Leverenz JB, Love S, Mackenzie IR, Mann DM, Masliah E, McKee AC, Montine TJ, Morris JC, Schneider JA, Sonnen JA, Thal DR, Trojanowski JQ, Troncoso JC, Wisniewski T, Woltjer RL, Beach TG (2012) Correlation of Alzheimer disease neuropathologic changes with cognitive status: a review of the literature. J Neuropathol Exp Neurol 71, 362–381. doi: 10.1097/NEN.0b013e31825018f7 [PubMed: 22487856]

Renier G, Clement I, Desfaits AC, Lambert A (1996) Direct stimulatory effect of insulin-like growth factor-1 on monocyte and macrophage tumor necrosis factor-α production. Endocrinology 137, 4611–4618. doi: 10.1210/2n,137.11.4611 [PubMed: 8895324]

Sperling RA, Alsen PS, BNeckett LA, Bennett DA, Craft S, Fagan AM, Iwatsubo T, Jack CR Jr., Kaye J, Montine TJ, Park DC, Reiman EM, Rowe CC, Siemers E, Stern Y, Yaffe K, Carrillo MC, Thies B, Morrison-Bogorad M, Wagster MV, Phelps CH (2011) Toward defining the preclinical stages of Alzheimer's disease: recommendation from the national Institute on Aging- Alzheimer's Association work groups on diagnostic guidelines. Alzheimers Dement 7, 280–292. doi: 10.1016/j.jalz.2011.03.003 [PubMed: 21514248]

Wang A, Anderson BM, Novakovic ZM, Grasso P (2018)[D-Leu-4]-OB3 and MA-[D-Leu-4]-OB3, small molecule synthetic peptide leptin mimetics, improve glycemic control in diet-induced (DIO) obesemice. Peptides 101, 51–59. doi: 10.1016/j.peptides.2017.12.012 [PubMed: 29269073]

Highlights

- MA-[D-Leu-4]-OB3 reduces neurodegeneration in mouse models of T1DM and T2DM
- MA-[D-Leu-4]-OB3 reduces serum TNF-α and IFG-1 in mouse models of T1DM and T2DM
- MA-[D-Leu-4]-OB3 improves cognitive function in mouse models of T1DM and T2DM
- MA-[D-Leu-4]-OB3 may have application to human AD, VaD, or mixed dementia

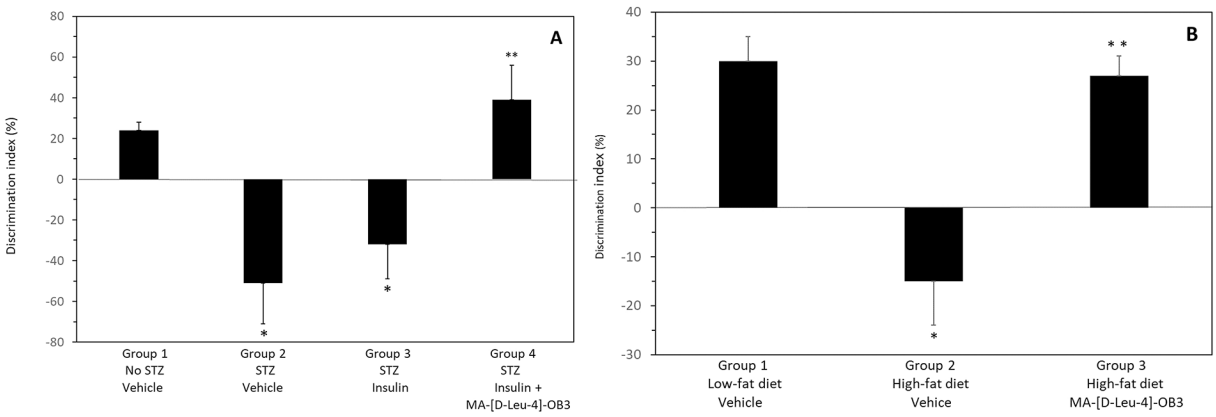

Fig. 1.

Effects of MA- [D-Leu-4]-OB3 on the discrimination index (DI) of male STZ-treated SW mice (Fig. 1A) and male C57BL/6J DIO mice maintained on a high-fat diet for 30 weeks (Fig. 1B). Each bar and vertical line represents the average DI of mice in each group (mean ∓ SEM, n = 8). *P < 0.05 compared to Group 1 (Fig 1A and 1B). **P > 0.05 compared Group 1 (Fig 1A and 1B).

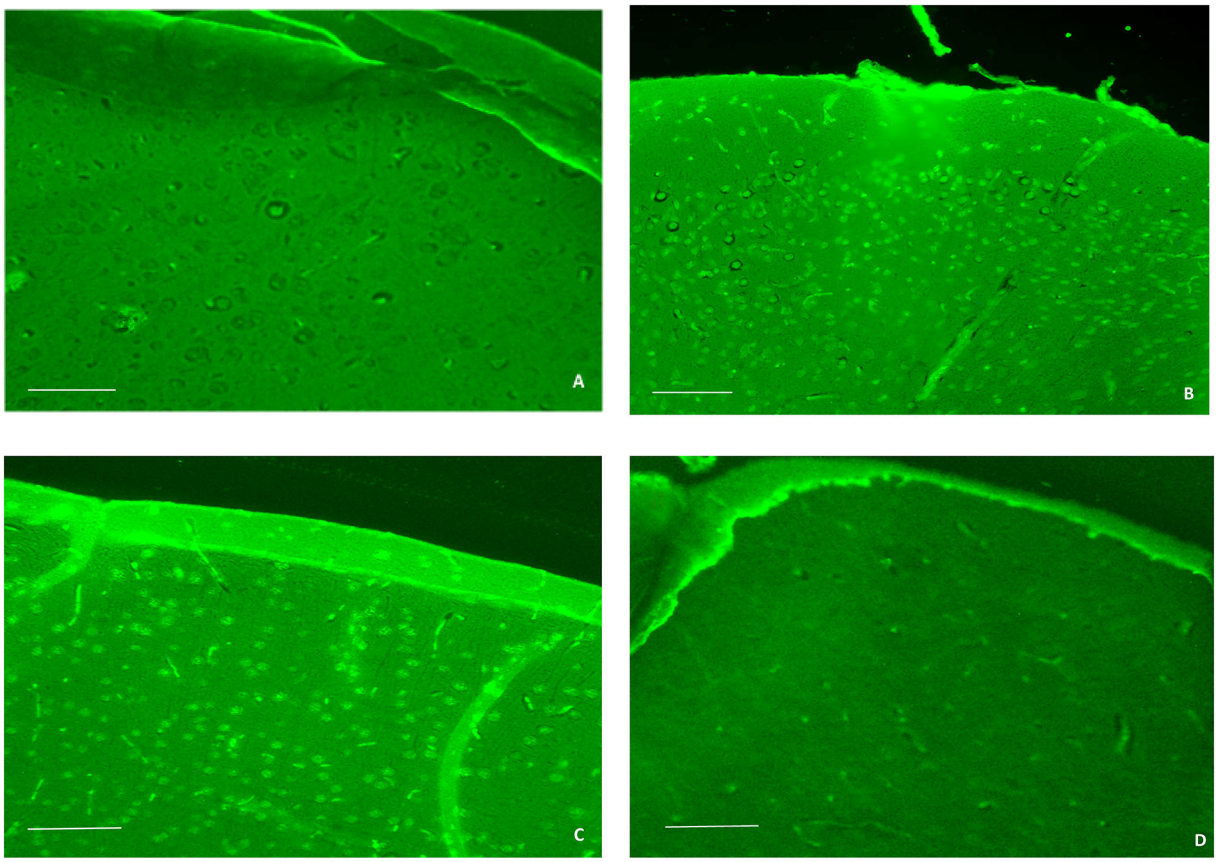

Fig. 2.

Representative images of the cerebral cortex of male wild-type SW mice (A), STZ-treated mice (B), STZ-treated mice given insulin alone (C), and STZ-treated mice given insulin in combination with MA-[D-Leu-4]-OB3 (D) for 17 days. FJC labeling of degenerating neurons was minimal in Fig. 2A, abundant in Fig. 2B and Fig. 2C, and significantly reduced in Fig, 2D. (scale bar = 100 μm)

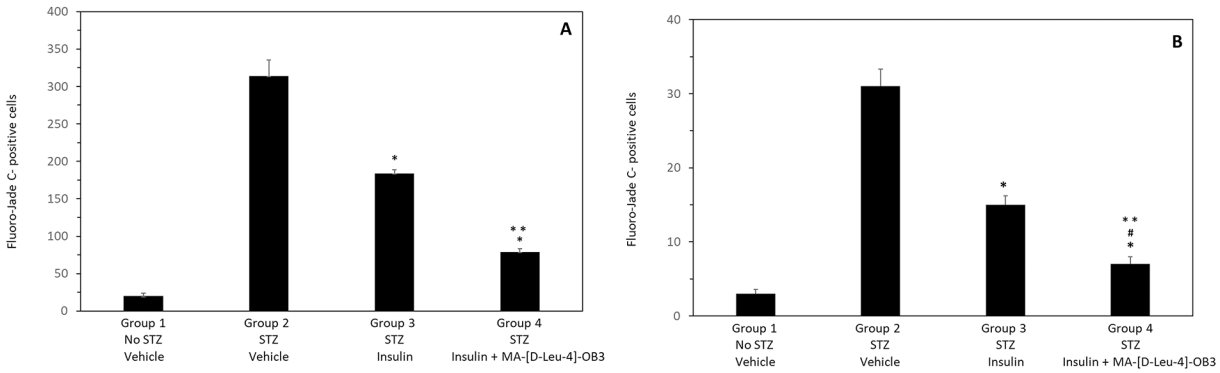

Fig. 3.

Quantification of the number of FJC-positive cells in the cerebral cortex (A) and hippocampus (B) of STZ-treated male SW mice given insulin alone or in combination with MA-[D-Leu-4]-OB3 for 17 days. Each bar and vertical line represents the average (mean ± SEM) number of degenerating cells counted in 10 fields from 4 mice in each treatment group. *P < 0.05 compared to Group 2 (Fig 3A and Fig 3B); ** P < 0.05 compared to Group 3 (Fig 4A and Fig 4B). $^{\#}$P > 0.05 compared to Group 1 (Fig 3B).

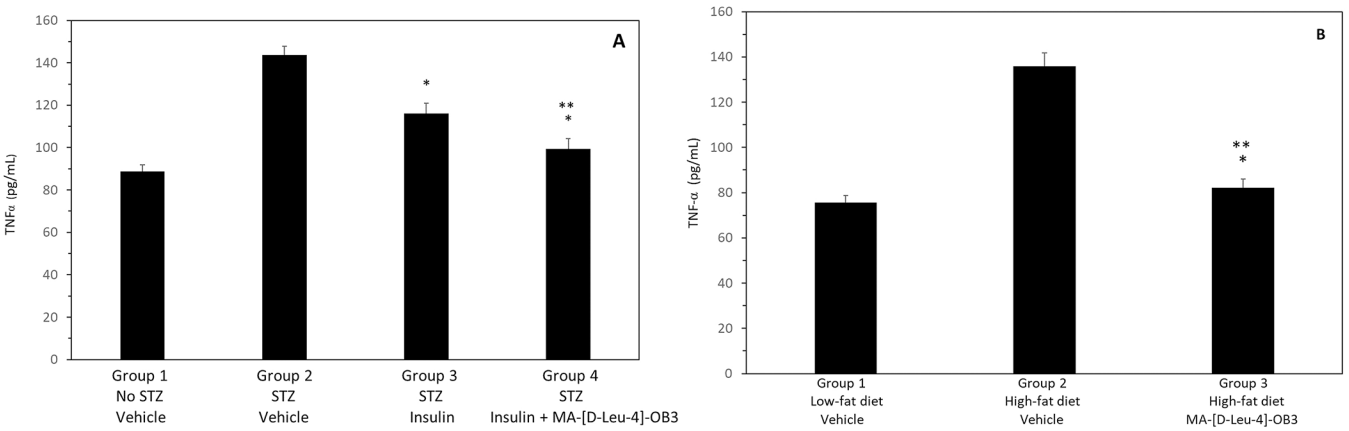

Fig. 4.

Effects of MA- [D-Leu-4]-OB3 on serum TNF-α levels in male STZ-treated SW mice (Fig. 4A) and C57BL/6J DIO mice maintained on a high-fat diet for 30 weeks (Fig. 4B). Each bar and vertical line represents the average serum TNF-α level of mice in each group (mean ± SEM, n = 8). *P < 0.05 compared to Group 2 (Fig 4A and Fig 4B). **P > 0.05 compared to Group 1 (Fig 4A and Fig 4B).

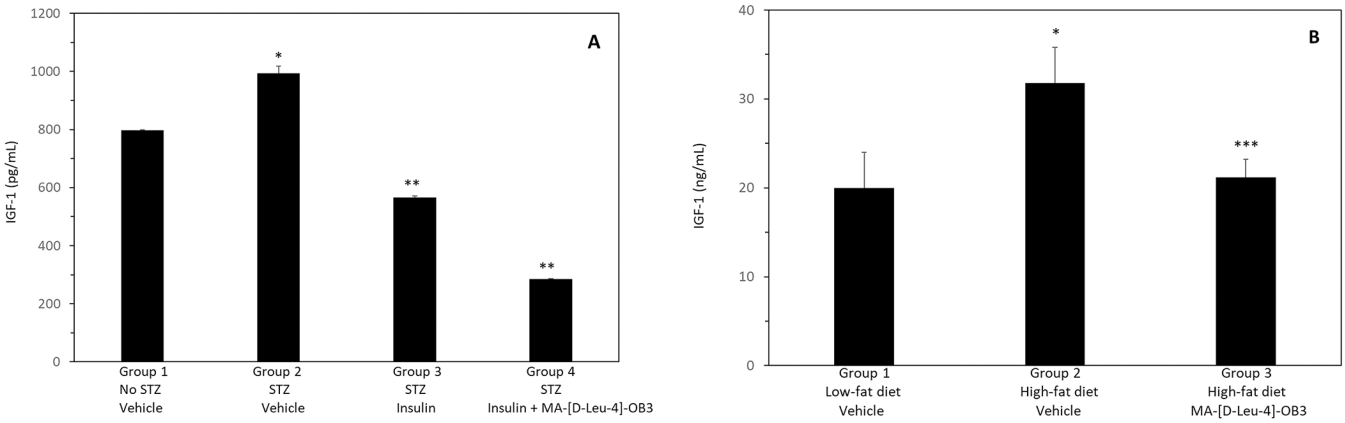

Fig. 5.

Effects of MA-[D-Leu-4]-OB3 on serum IGF-1 levels in male STZ-treated SW mice (Fig. 5A) and C57BL/6J DIO mice maintained on a high-fat diet for 30 weeks (Fig. 5B). Each bar and vertical line represents the average serum IGF-1 level of mice in each group (mean ± SEM, n = 8). *P < 0.05 compared Group 1 (Fig 5A and 5B). **P < 0.05 compared to Group 2 (Fig 5A). ***P > 0.05 compared Group 1 (Fig 5B).

Table 1.

Effects of MA-[D-Leu-4]-OB3 (16.6 mg/kg, oral gavage) on glycemic control in mouse models of T1DM (STZ-induced) and T2DM (DIO, diet induced obese)

T1DM[a]	Group 1 No STZ Vehicle	Group 2 STZ Vehicle	Group 3 STZ Insulin (0.05U)	Group 4 STZ Insulin (0.05U) + MA-D-Leu-4]-OB3
Initial body (gm)	31.3 ± 0.7	31.4 ± 0.6	31.8 ± 0.5	31.5 ± 0.9
Final body weight (gm)	35.0 ± 0.8[c]	33.4 ± 1.2[c]	37.4 ± 0.8[c]	32.6 ± 0.8
Change (gm)	+3.7	+2.0	+5.6	+1.1
Initial fasting blood glucose (mg/dL)	149 ± 7	278 ± 55	302 ± 37	325 ± 52
Final fasting blood glucose (mg/dL)	162 ± 4	530 ± 52[d]	280 ± 47	189 ± 8[d]
Change (mg/dL)	+13	+252	−22	−135
T2DM[b]	Group 1 C57BL/6J Low-fat diet Vehicle	Group 2 DIO High-fat diet Vehicle	Group 3 DIO High-fat diet MA-[D-Leu-4]-OB3	
Body weight (gm)	37 ± 0.7	52 ± 0.9	56 ±1.0	
Initial AUC (mg/dL × min)	13,636 ± 756	20,099 ± 882[e]	23,714 ± 1207[e]	
Final AUC (mg/dL × min)	12,783 ± 283	18,941 ± 365[e]	12,226 ± 545[f]	
Change (mg/dL × min)	−853	−1158	−11,488	

[a] Data taken from Anderson et al., 2019

[b] Data taken from Hirschstein et al., 2019

[c] $P < 0.05$ compared to initial body weight

[d] $P < 0.05$ compared to initial fasting blood glucose

[e] $P < 0.05$ compared to Group 1

[f] $P > 0.05$ compared to Group 1